Comet 17P/Holmes: A Megaburst Survivor

Zdenek Sekanina

Jet Propulsion Laboratory; California Institute of Technology; Pasadena, CA 91109; U.S.A.

Abstract. *The light curve of comet 17P/Holmes in 2007-2009 — before, during, and after the megaburst — is compared with the light curves at previous apparitions. The comet has remained about 4 magnitudes brighter in the late 2008 and early 2009 relative to 1986-2000, indicating the presence of lingering or replenished particulate debris in the atmosphere. Observed brightness variations during the active phase of the megaburst and along the protracted plateau offer the event's improved parameters, all closely confirming the preliminary values in Sekanina (2008a). Modeling the steep brightness increase during the active phase allows a determination of temporal variations in the mass rate of dust injected into the halo during the megaburst. The curve is sharply peaked, with a maximum rate of 2 × 10^9 g/s (!) about 0.9 day after the event's onset, yet the halo is optically thin. A moderate outburst had evidently preceded the main event, overlapping it partially. This evidence, diagnostic of ongoing fragmentation, supports the physical scenario in Sekanina (2008a). The comet's post-megaburst behavior mimics, on a grandiose scale, its behavior following the two 1892-1893 explosions. Evidence is presented for an outburst in 1899, possibly related to the events one revolution earlier, and for elevated activity throughout 1899 and 1906. Comet 17P/Holmes is expected to be distinctly brighter at upcoming returns to the sun and could become an "annual" comet.*

1. Introduction

In late October 2007, comet 17P/Holmes underwent an enormous explosion or *megaburst*, during which the brightness increased by nearly a million times in two days. It is desirable to learn, by continuing to monitor the light curve, about the further evolution of the comet as a survivor of the unrivaled explosive event. About 2000 total magnitude observations collected in the *International Comet Quarterly (ICQ)* and other complementary data available from the current apparition allow one to make conclusions on the comet's physical behavior and to compare it with its behavior during previous returns to the sun.

The terminology introduced and applied in two recent papers (Sekanina 2008a = Paper 1 and Sekanina 2008b = Paper 2) is used below. An observed magnitude of the comet, corrected — to the extent possible — for personal and instrumental bias (including a bandpass correction) and referred to a geocentric distance Δ of 1 AU by a Δ^{-2} law, is described by a normalized magnitude H_Δ. When referred to a heliocentric distance r of 1 AU by an r^{-2} law, this magnitude is called an intrinsic magnitude H_0. A phase effect, whose magnitude is not known for comet 17P/Holmes, has been included in neither H_Δ nor H_0, but it is estimated in Sec. 5. Unlike in Paper 2, where I applied Divine *et al.*'s (1986) generic law, phase-correction estimates are now based on Marcus' (2007) recent work.

2. The History of Detection of Comet 17P/Holmes

Much insight into the comet's activity over long periods of time is gained by compiling information on the first and the last observation of 17P/Holmes at each of its apparitions. A synopsis of such data, presented in Table 1, provides information on long-term variations in the comet's behavior.

Although the times of the first and last observations are known to be affected by changing geometry due to the comet's motion relative to the sun and earth, differences on a time scale exceeding the duration of a conjunction gap (say, 4-5 months) cannot be explained in this way. Column 8 of Table 1, which lists the time of the last observation relative to perihelion, shows that before 2007 the comet had *never* been observed more than one year after perihelion. At the 2007 apparition, the comet has already been observed for nearly two years after perihelion, with monitoring still continuing. The predicted motion in the sky suggests that the comet could be under observation until May-June 2009 and that its imaging may resume again before the end of 2009 (Sec. 3).

The return of 2007 also holds a record in terms of the time spanned by the observations. The apparition of 2000 is a close second thanks only to the single-night imaging with the ESO's 360-cm telescope nearly one year before perihelion (Leisy 1999). A second observation followed fully 13 months later.

Table 1 also shows that, at the 1892, 1899, and 1906 apparitions, the comet was observed longer after perihelion than in 1993 — even though the orbital geometries, especially in 1899 and 1993, were rather similar, with the perihelion passages at the two returns occurring within three weeks of each other. And while the largest refractors in existence were employed to observe the comet in 1899, the telescopic equipment used in 1993 was clearly superior. It is tempting to attribute the long post-perihelion arcs of observation at the first three apparitions, but especially in 1899, to a greater intrinsic brightness of the comet caused by lingering effects of the outbursts in 1892-1893. This conjecture is examined more closely in the following section using available information on the observed light curves.

Table 1. History of observations of comet 17P/Holmes (apparitions 1892–2007).

Apparition No.	Time of perihelion (UT)	First observation		Last observation		From perih. (days)[b]			References[c]
		Date (UT)	Mag.[a]	Date (UT)	Mag.[a]	first	last	span	
1	1892 Jun. 13.95	1892 Nov. 6.99	n.e.(T,v)	1893 Mar. 16.83	11.5(T,v)	+146.0	+275.9	129.9	1–7[d]
2	1899 Apr. 28.59	1899 Jun. 11.46	16(T,v)	1900 Jan. 21.26	16(T,v)	+21.0	+267.7	246.7	8,9
3	1906 Mar. 14.70	1906 Aug. 29.05	15.5(T,p)	1906 Dec. 7.77	16(T,p)	+167.4	+268.1	100.7	10–12
4	1964 Nov. 15.93	1964 Jul. 16.31	19.2(N,p)	1965 Jan. 2.13	18.8(N,p)	−122.6	+47.2	169.8	13
5	1972 Jan. 30.82	1971 Jun. 20.39	~20.0(N,p)	1973 Jan. 30.25	20.6(N,p)	−224.4	+365.4	589.8	14–16
6	1979 Feb. 22.66	1979 Jul. 20.30	19.5(N,p)	1980 Feb. 11.10	.....	+147.6	+353.4	205.8	17,18[e]
7	1986 Mar. 14.13	1986 Jun. 9.46	18(T,c)	1986 Dec. 29.31	18.2(T,c)	+87.3	+290.2	202.9	19,20
8	1993 Apr. 10.74	1993 May 24.77	18(T,p)	1993 Oct. 20.41	.....	+44.0	+192.7	148.7	21–24[f]
9	2000 May 11.82	1999 Jun. 7.21	20.9(T,c)	2001 Feb. 20.53	18.6(T,c)	−339.6	+284.7	624.3	25–27[g]
10	2007 May 4.50	2007 May 13.45	15.9(N,c)	2009 Feb. 28.92	19.3(T,c)	+9.0	+666.4	657.4	28,29[h]

[a] The observed magnitude is T = total (a.k.a. m_1) or N = "nuclear" (a.k.a. m_2) and was obtained either visually (v) or photographically (p) or with use of CCD, a charge-coupled device (c); n.e. refers to naked-eye visibility, dots indicate that no magnitude was reported.

[b] When a time of the first observation is negative, the comet was detected before perihelion; a positive time of the first or the last observation refers to a post-perihelion sighting; the time difference between the two observations is in column *span*.

[c] References: 1 = Holmes (1892); 2 = Copeland (1893); 3 = Barnard (1896); 4 = Barnard (1913); 5 = Backhouse (1902); 6 = Bobrovnikoff (1943); 7 = Kobold (1893); 8 = Perrine (1899); 9 = Perrine (1900); 10 = Wolf (1906a); 11 = Wolf (1906b); 12 = Wolf (1907); 13 = Roemer and Lloyd (1966); 14 = Roemer (1971); 15 = Roemer (1973); 16 = Roemer (1981); 17 = Shao and Schwartz (1979); 18 = McCrosky *et al.* (1980); 19 = Gibson (1986); 20 = Scotti (1987); 21 = Seki (1993); 22 = Balam and Tatum (1993); 23 = Nakamura (1993); 24 = Nakamura (1994); 25 = Leisy (1999); 26 = Oribe (2001); 27 = Jäger (2000); 28 = Guido *et al.* (2007); 29 = Hasubick (2009).

[d] Not much information on his observation is offered by the discoverer in Ref. 1; the time of first detection is listed in Ref. 2; a brightness estimate (beyond a remark in Ref. 1 that the comet was seen with the naked eye), based on Barnard's accounts (Refs. 3–4) made within a few days after discovery, suggests that the comet could hardly be brighter than magnitude 5 on November 6. The last meaningful observation was made by Backhouse (Ref. 5) with an 11-cm refractor (see also Ref. 6); Kobold (Ref. 7) remarked, however, that "on April 6 the comet was, after a long search, discerned as an extremely dim flickering trace of light, but no observation on this and several subsequent evenings was possible" with the 46-cm refractor of the Strasbourg Observatory and he reported no magnitude for April 6; this date is ~297 days past perihelion, thus extending the span of marginal detection to ~151 days.

[e] No magnitude was reported by McCrosky *et al.* (Ref. 18) for their observation on February 11, 1980.

[f] No magnitude was reported by Balam and Tatum (Ref. 22) for their observation on October 20, 1993. Less than one day before this last observation, Nakamura (Refs. 23 and 24) found the comet to be of total magnitude 17.7, using a 60-cm Ritchey-Chrétien reflector and a CCD detector.

[g] Following the recovery observation with the 360-cm reflector at the La Silla Station of the European Southern Observatory (Ref. 25), the comet was not sighted again for the next 13 months, until Jäger (Ref. 27) observed it photographically as an object of total magnitude 15.0 on July 6 and 7, 2000, some 55–56 days after perihelion.

[h] The most recent observation as of the end of February 2009.

◇ ◇ ◇

3. The Light Curve

As in Papers 1 and 2, a light curve is understood to be a plot of the normalized magnitude H_Δ against time that is reckoned from perihelion. For the current apparition, the *ICQ* was the primary data source, but numerous issues of the *Minor Planet Electronic Circular* (*MPEC*) were a secondary source, especially in the pre-explosion and post-plateau time intervals. Only magnitudes referred to as *total* (T) by the observers in the *MPECs* were considered for inclusion in our data set. The magnitudes were tested for consistency and corrected (where possible) for personal and instrumental effects, as explained in Paper 1. The data from the apparitions starting with 1986 were described in Paper 1. A few comments follow on some new data (published after completion of Paper 1) from the current apparition and on brightness estimates from the apparitions 1892-1906. No total magnitudes are available from the apparitions of 1964, 1972, and 1979.

Figure 1 presents comprehensive information on the history of the post-perihelion light curve of comet 17P/Holmes. For the current return, the light curve is based on more than 1500 magnitude estimates and clearly shows four phases of brightness evolution: (i) an initial *"quiescent" phase*, with the comet relatively faint; shortly after perihelion it was brighter than at previous apparitions but fading more rapidly; (ii) an *active phase* of the megaburst, with explosive brightening; (iii) a *post-outburst plateau*, with the comet's brightness very slowly subsiding with time; and (iv) *distinct fading* resulting in a new, *elevated* quasi-quiescent state.

The last pre-conjunction observations from late March and April 2008 (320 to 360 days after perihelion) clearly show a progressively increasing deviation of the light curve from the prediction for a hypothetical loss-free halo (Figure 1), when

no dust escapes. Consequently, it came as no surprise that the comet was much fainter when it was recovered, some 500 days after perihelion, in the second half of 2008, following conjunction with the sun. But when the post-conjunction data were normalized, the comet turned out to be about 4 magnitudes brighter than indicated by the linearly extrapolated light curve from the apparitions 1986-2000, when the comet must have been very little, if at all, active at 4 AU from the sun and beyond. In fact, measured by the normalized magnitude H_Δ, the comet was brighter $\sim$ 600 days after its 2007 perihelion than $\sim$ 300 days after perihelion in 1986, when it was still slightly brighter than in 1993 and 2000. The large brightness excess nearly two years after perihelion raises the question of possible long-term effects of the 2007 megaburst on the evolution of the comet during its future returns to the sun. One may recall that a similarly elevated brightness, lingering over at least two revolutions about the sun, was exhibited by comet 73P/Schwassmann-Wachmann after it had split in 1995 (Paper 1).

◇ ◇ ◇

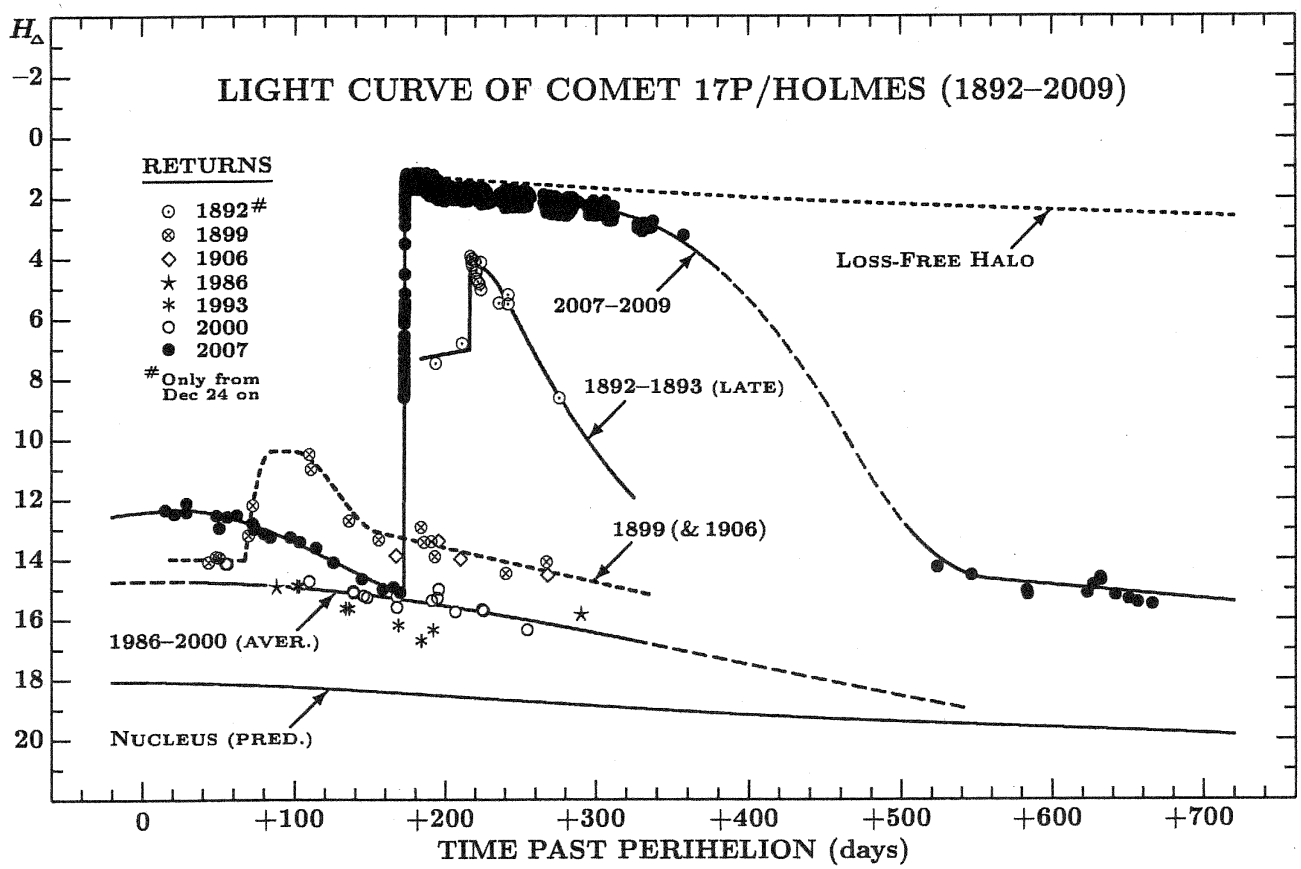

Figure 1. Light curves of comet 17P/Holmes at seven apparitions. The magnitudes H_Δ, normalized to a unit geocentric distance, have been, where possible, corrected for personal and instrumental effects. The observations are represented by apparition-specific symbols. Note the post-megaburst plateau persisting in 2007–2008. The hypothetical loss-free halo shows the expected light curve in a case, when no dust particles injected into the halo during the megaburst escape. The bottom curve is a predicted normalized magnitude, at a zero phase angle and a geometric albedo of 0.04, of a spherical nucleus 3.3 km in diameter.

◇ ◇ ◇

Inspired by this finding, I set up to investigate, as a potential precedent, the comet's behavior in a latter part of the 1892 apparition and during the apparitions of 1899 and 1906. This decision was in part also prompted by the conclusions in Sec. 2.

At the first apparition of 17P/Holmes, only the portion of the light curve from 1892 December 24 on has been plotted, a time slot that covers the January 1893 outburst and the comet's final fading. I resorted to the data set collected by Bobrovnikoff (1943) for most observations, including those made by T. W. Backhouse with the naked eye, binoculars, and an 11-cm refractor; by E. E. Barnard with an 8-cm seeker; by J. Holetschek with a 4-cm seeker; and by A. Kammermann with a 25-cm refractor. Referring the magnitudes to Barnard's naked-eye data from November 1892 and applying personal and instrumental corrections, I obtained a light curve that looks like a compressed version of the 2007 light curve. The peak intrinsic magnitude of the January 1893 outburst is $(H_0)_{\rm peak} = 1.8$, or 0.6 magnitude fainter than adopted in Paper 1, suggesting a fairly large uncertainty in the magnitude scale employed. The final magnitude observation, on 1893 March 16 (Backhouse 1902, Bobrovnikoff 1943), obtained when the comet was about 276 days after perihelion at a heliocentric distance of 2.88 AU, indicates a steeply declining light curve. Even if Backhouse did not

underestimate the brightness, the comet was then still about 1000 times brighter than at the same distance from the sun after perihelion in 1986-2000 (Figure 1).

In 1899 the comet, fainter than during the first apparition, was detected by three observers only: Perrine (1899, 1900), Aitken (1900), and Barnard (1932).[1] However, only Perrine and Barnard published magnitudes for specific dates. The comet must have undergone another outburst, which commenced probably on July 4, about 67 days after perihelion. Although accompanied by no dust halo and, to my knowledge, never before reported explicitly as an outburst, this event is apparent from the linked observations by Perrine in June-July and by Barnard in August, and its existence seems to be well established.

According to Perrine, the comet was not brighter than magnitude 16 when recovered on 1899 June 11 UT, with only a slight brightening at the center. It was of about the same brightness on June 16, 17, and 18, but brightened to magnitude 15 on July 7 and to magnitude 14 on July 10 UT, when it had a faint nucleus. On July 15 and 16 UT, the sky was hazy and smoky, yet Perrine noticed that the comet was still brighter at the center on the latter night. When, after a wide gap, he resumed his observations on October 1 UT, the comet was again brighter at the center and of magnitude 14.5, but had no nucleus.

Barnard began his observations on August 16 UT, estimating the comet's magnitude as 13. The next night the magnitude was 13.5 and the comet showed a feeble nucleus. Barnard reported the comet's slow fading in September through November. Between October 31 and November 5 UT, he estimated the comet to be of magnitude 15-16, while Perrine between October 29 and November 7 UT recorded magnitude 14-15. This suggests that Barnard, observing with the 102-cm refractor of the Yerkes Observatory, underestimated the brightness by $\sim$ 1 magnitude relative to Perrine, who used the 91-cm refractor of the Lick Observatory. The difference in the normalized brightness H_Δ between Perrine's estimates before July 7 and Barnard's corrected brightest estimate on August 16 is 3.4 magnitudes, so the amplitude of the outburst may have been close to 4 magnitudes, if not more. The post-outburst light curve in 1899 runs consistently about 1.7 magnitudes above the 1986-2000 light curve (Figure 1). If Perrine underestimated the *total* brightness, the comet may have been more than 2 magnitudes brighter in 1899 than in 1986-2000 — and at its peak brightness, in mid-July 1899, it should not have been fainter than $(H_0)_{\rm peak} \simeq 8$. The comet's 1899 light curve thus exhibits clear signs of lingering effects of the 1892-1893 events.

In 1906, the comet was observed photographically by Wolf (1906a, 1906b, 1906c, 1906d, 1906e, 1907) four times between $5\frac{1}{2}$ and $9\frac{1}{2}$ months after perihelion. Since Wolf (1892) calibrated his photographic magnitudes using star catalogues based on visual-magnitude scales, no color correction was applied to his reported magnitudes. There is a fairly good correspondence between Perrine's 1899 visual magnitudes and Wolf's 1906 photographic magnitudes in the shared part of the light curve in Figure 1, even though Wolf's underestimating the brightness is equally as possible as Perrine's. In any case, the comet's behavior in 1906 appears to have been affected by the 1892 events just like its behavior in 1899.

The conclusion from this exercise is that lingering effects of the 2007 megaburst should make comet 17P/Holmes distinctly brighter at its future returns to the sun — at least in 2014 and 2021 — than in 1986-2000. Extrapolation of the 2008-2009 post-conjunction light curve from Figure 1 suggests that, during its near-aphelic opposition with the sun in March 2011, the comet could be as bright as apparent magnitude 20 and become — at least for a few revolutions about the sun — an "annual" comet, observable all around the orbit, like 2P/Encke, 29P/Schwassmann-Wachmann, 65P/Gunn, and others (e.g., Marsden 1973, 1985).

4. The Megaburst of 2007 and Its Aftermath

The apparent nuclear magnitude 8.4, initially reported as the comet's brightness at the time of discovery of the megaburst on 2007 October 24.067 UT, and the rapid brightening in subsequent hours (Henriquez Santana 2007) showed that this event had been detected soon after its onset. More recent communications by Hsieh *et al.* (2007), by Henriquez Santana (2008), and by Trigo-Rodríguez *et al.* (2008) provided data that extended the coverage of the megaburst closer to its onset and also improved the data set, which makes it now possible to model temporal variations in the dust-injection rate during the active phase (Sec. 6). Hsieh *et al.* detected the megaburst first on October 23.99 UT, and Henriquez Santana's first frame (with the comet's image saturated) was taken on October 23.945 UT.

In Paper 1, the onset time of the megaburst, $t_{\rm beg}$, was determined by extrapolating back in time the observed dimensions of the sharply-bounded, expanding dust halo. Finding for the onset time October 23.7 $\pm$ 0.2 UT, or 172.2 days after perihelion, I used this technique to determine also the rate at which the halo was uniformly expanding in the early period and the total mass of injected dust, which turned out to be more than 1 percent of the comet's mass (Paper 1). The magnitudes are less helpful in an effort to derive the onset time, unless one carries out a comprehensive analysis of the light curve during the active phase of the megaburst (Sec. 6). It is noteworthy, however, that from photometry of images taken with the SuperWASP-North robotic facility on La Palma, Canary Islands, between October 23.99 and 24.10 UT, Hsieh *et al.* (2007) calculated, on the assumption of an optically thick dust halo, that the event began on approximately October 23.8 UT, or 172.3 days after perihelion, in excellent agreement with the determination based on halo expansion.

Recent additional magnitude reports referring to the pre-megaburst period of time have improved the quality of the light curve in this period of time (Figure 1) and allowed one to determine with fair accuracy the normalized and intrinsic magnitudes at the event's onset. For October 23.7 UT, one finds $(H_\Delta)_{\rm onset} = 15.19 \pm 0.10$ and $(H_0)_{\rm onset} = 13.26 \pm 0.10$, equivalent to an apparent visual magnitude of 16.26, corrected for personal and instrumental effects (but with no

[1] After Barnard's death in 1923, G. Van Biesbroeck edited and prepared for publication two papers containing Barnard's previously unreported Yerkes observations made between 1898 and 1913; this reference is to the first of those two papers.

phase correction; see Sec. 5). This scenario is consistent with an upper limit of magnitude 15, implied by the failure of the SuperWASP-North facility to detect the comet on October 23.27 UT (Hsieh *et al.* 2007).

◇ ◇ ◇

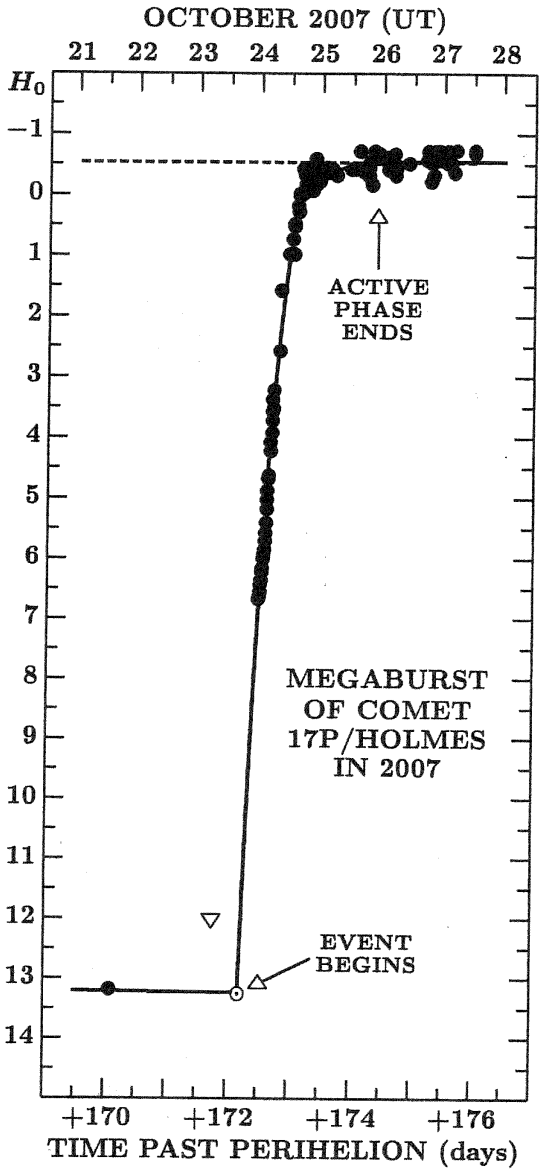

Figure 2. Close-up view of the temporal variations in the intrinsic magnitude H_0 during the active phase of the 2007 megaburst of comet 17P/Holmes. The fitted curve is an empirical polynomial. Most data in the early part of the curve are subset averages of 141 magnitudes from unsaturated frames obtained by Henriquez Santana (2008) between October 24.001 and 24.136 UT. The transition of the active phase, whose onset and end are marked, to a long plateau of constant brightness, is seen in the upper right of this figure. The bullet on the curve of H_0 at the lower left is K. Kadota's observation made on October 21.60 UT. The down-pointing triangle is a nondetection by Hsieh et al. (2007) on October 23.27 UT.

◇ ◇ ◇

Along the steeply increasing light curve of the early active phase of the megaburst, Henriquez Santana (2008) took 226 frames of the comet. On 141 of these frames, the comet image is unsaturated, and I divided them into 14 subsets and calculated the averages, which make up most of the data points near the lower ends of the light curve in Figure 1 and the curve of intrinsic magnitude H_0 in Figure 2. These H_0 averages have been calibrated using the V magnitudes by Hsieh *et al.* (2007) and combined with additional magnitude estimates from a variety of published sources, which make up the upper end of the curve in Figure 2. No magnitudes from Henriquez Santana's saturated images have been incorporated into Figures 1 and 2. The problem of modeling the curve of rapid intrinsic brightening during the active phase of the megaburst is addressed in Sec. 6.

I remarked in Paper 1 that the termination point of the active phase is determined by the time the post-explosion plateau is first reached on the plot of H_0 against time. The transition between the active phase and the plateau is clearly seen in Figure 3, which is a variation of Figure 4 from Paper 1. While the plot in Paper 1 contained 92 data points between October 25.5 and November 3.0 UT, or 174 and 182.5 days after perihelion, the updated investigation of the post-outburst plateau in this paper is based on 582 data points between October 24.5 and November 13.5 UT, or 173 and 193 days after perihelion.

The intrinsic magnitudes of 17P/Holmes averaged over consecutive intervals of 0.5 day in the 20-day time period are listed, together with their mean errors, in Table 2. The numbers of data points per interval vary from 4 to 33, as shown in columns 3 and 6. These magnitude averages have been used to determine three parameters of the comet's light curve: (i) the time of termination of the active phase of the megaburst; (ii) the peak intrinsic magnitude; and (iii) the period

of time over which the plateau retained, within the errors of observation, the peak intrinsic brightness.

◇ ◇ ◇

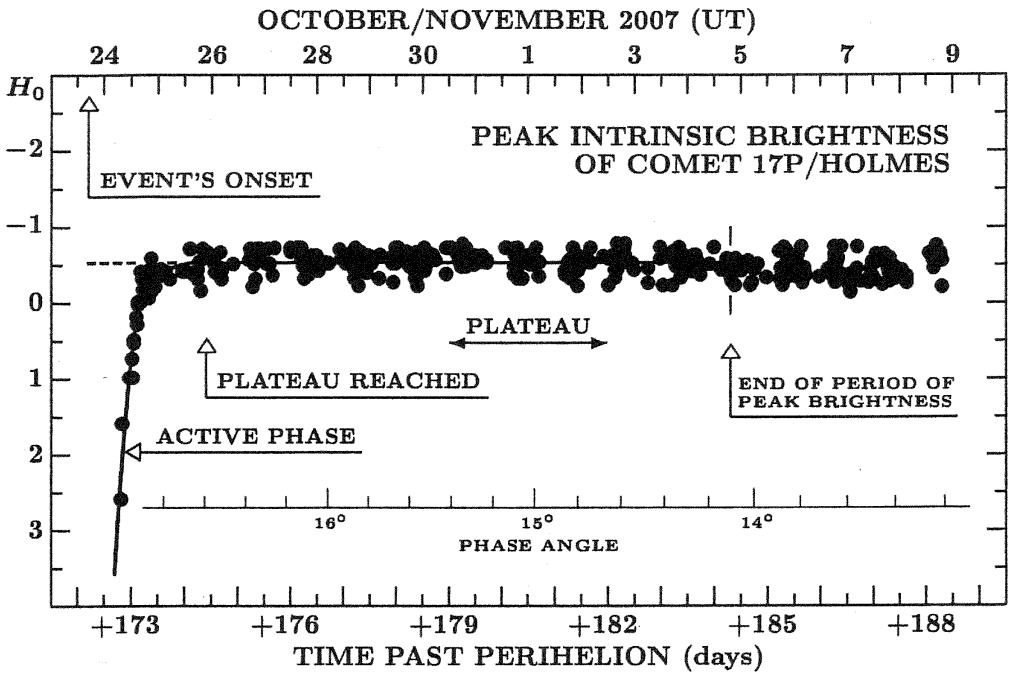

Figure 3. Close-up view of the temporal variations in the intrinsic magnitude H_0 following the active phase of the 2007 megaburst of comet 17P/Holmes. The peak intrinsic magnitude $(H_0)_{peak} = -0.53 \pm 0.12$ has been calculated from 291 magnitude estimates that make up the flat portion of the plateau, between 174.4 and 184.3 days after perihelion, or between October 25.9 and November 4.8 UT. These boundaries have been determined in part from the sets of averaged values of H_0 in Table 2. The beginning of the plateau with the peak intrinsic brightness coincides with the termination time of the active phase of the megaburst. Variations in the phase angle are also shown.

◇ ◇ ◇

Table 2. Averaged intrinsic magnitude H_0 of comet 17P/Holmes on the plateau after the megaburst.

Range of times past perihelion, $t-T$ (days)[a]	Intrinsic magnitude, H_0 (mag)	Number of data points	Range of times past perihelion, $t-T$ (days)	Intrinsic magnitude, H_0 (mag)	Number of data points
173.01 – 173.50	-0.07 ± 0.38	28	183.01 – 183.50	-0.49 ± 0.13	28
173.51 – 174.00	-0.38 ± 0.04	7	183.51 – 184.00	-0.50 ± 0.12	10
174.01 – 174.50[b]	-0.47 ± 0.18	13	184.01 – 184.50[c]	-0.42 ± 0.11	12
174.51 – 175.00	-0.48 ± 0.11	8	184.51 – 185.00	-0.39 ± 0.12	7
175.01 – 175.50	-0.56 ± 0.17	11	185.01 – 185.50	-0.46 ± 0.14	24
175.51 – 176.00	-0.58 ± 0.14	8	185.51 – 186.00	-0.45 ± 0.15	10
176.01 – 176.50	-0.52 ± 0.10	22	186.01 – 186.50	-0.49 ± 0.14	15
176.51 – 177.00	-0.53 ± 0.09	6	186.51 – 187.00	-0.35 ± 0.15	14
177.01 – 177.50	-0.50 ± 0.14	15	187.01 – 187.50	-0.45 ± 0.12	22
177.51 – 178.00	-0.51 ± 0.15	9	187.51 – 188.00	-0.33 ± 0.07	7
178.01 – 178.50	-0.52 ± 0.11	27	188.01 – 188.50	-0.44 ± 0.15	17
178.51 – 179.00	-0.56 ± 0.11	16	188.51 – 189.00	-0.20 ± 0.12	5
179.01 – 179.50	-0.56 ± 0.09	28	189.01 – 189.50	-0.31 ± 0.10	12
179.51 – 180.00	-0.55 ± 0.03	8	189.51 – 190.00	-0.28 ± 0.11	5
180.01 – 180.50	-0.56 ± 0.11	33	190.01 – 190.50	-0.34 ± 0.16	21
180.51 – 181.00	-0.57 ± 0.11	10	190.51 – 191.00	-0.37 ± 0.17	17
181.01 – 181.50	-0.49 ± 0.11	22	191.01 – 191.50	-0.35 ± 0.16	31
181.51 – 182.00	-0.54 ± 0.15	7	191.51 – 192.00	-0.31 ± 0.27	5
182.01 – 182.50	-0.55 ± 0.14	13	192.01 – 192.50	-0.43 ± 0.16	18
182.51 – 183.00	-0.49 ± 0.20	4	192.51 – 193.00	-0.37 ± 0.20	7

[a] Time $t-T = 173.01$ days corresponds to 2007 Oct. 24.51 UT; $t-T = 193.00$ days, to 2007 Nov. 13.50 UT.
[b] This interval covers the probable time of termination of the active phase of the meagburst.
[c] This interval covers the probable end of the period of peak intrinsic brightness.

These parameters have been calculated iteratively. First, for a selected set of intrinsic magnitudes at times just before a visually estimated end of the active phase of the megaburst in Figure 3 and Table 2, a least-squares polynomial approximation to their temporal variation is fitted and used to calculate, from the condition of $dH_0(t)/dt = 0$, the time t_{peak}, at which the plateau is first reached and the corresponding peak intrinsic magnitude $(H_0)_{peak}$. A time t_{down}, at which the brightness along the plateau begins to decline, is then estimated from Table 2, and a statistically averaged value of the peak intrinsic magnitude $(H_0)_{stat}$ is calculated from all data points between t_{peak} and t_{down}. If $(H_0)_{stat}$ does not coincide with $(H_0)_{peak}$, a new set of intrinsic magnitudes near the end of the active phase is selected, a least-squares polynomial approximation is fitted, t_{peak} and $(H_0)_{peak}$ calculated, and the iteration repeated. It should be noted that t_{peak}, the time the plateau is first reached, is identical with t_{end}, the termination time of the active phase of the megaburst.

◇ ◇ ◇

Table 3. Parameters for the 2007 megaburst of comet 17P/Holmes.

Parameter	Resulting value
Active phase	
Time of onset, t_{beg} (days after perihelion)[a]	172.2 ± 0.2
Nominal date of onset (2007 UT)[a]	October 23.7
Time of termination, t_{end} (days after perihelion)	174.4 ± 0.2
Nominal date of termination (2007 UT)	October 25.9
Duration (days)	2.2 ± 0.3
Intrinsic magnitude at onset, $(H_0)_{pre}$ (mag)	13.26 ± 0.10
Intrinsic magnitude at termination, $(H_0)_{peak}$ (mag)	-0.53 ± 0.12
Amplitude of the megaburst (mag)	13.79 ± 0.16
Relative increase in the comet's brightness	$328{,}000 \pm 48{,}000$
Total mass of dust injected into the halo, $\mathcal{M}_0$ (g)[a]	10^{14}
Plateau with peak intrinsic brightness	
Time when first reached, t_{peak} (days after perihelion)[b]	174.4 ± 0.2
Nominal date of t_{peak} (2007 UT)	October 25.9
Time when intrinsic brightness began to decline, t_{down} (days after perihelion)	184.3 ± 0.5
Nominal date of t_{down} (2007 UT)	November 4.8
Duration (days)	9.9 ± 0.5
Peak intrinsic magnitude[c], $(H_0)_{peak}$ (mag)	-0.53 ± 0.12

[a] From Paper 1; time t_{beg} is correlated with the halo's expansion velocity $v_{exp} = 0.50 \pm 0.02$ km/s.
[b] Identical with the time of termination of the active phase.
[c] Identical with the intrinsic magnitude at termination of the active phase.

◇ ◇ ◇

The final values for the parameters of the active phase and plateau, listed in Table 3, show that the peak intrinsic magnitude, -0.53 ± 0.12, is identical with its preliminary value in Paper 1, while the amplitude of the megaburst, that is, the difference between $(H_0)_{onset}$ and $(H_0)_{peak}$, and the duration of the active phase, that is, the time span between t_{beg} and t_{end}, have changed only marginally, within the errors of determination. The peak intrinsic magnitude in Table 3 was calculated from 291 data points, mostly naked-eye estimates.

5. Phase Effects

Deriving the brightness parameters in Sec. 4, I ignored effects due to the phase angle, sun-comet-earth. Because of the large perihelion distance of 17P/Holmes, the phase angle can never exceed 28°, so that the contribution from the phase law is restricted to near-backscattering effects. While the optical properties of cometary dust depend on its composition and particle-size distribution and remain unknown for comet 17P/Holmes, the phase effect can be approximated by employing the results for other comets. In his recent work, focused primarily on forward scattering by cometary dust and its fitting by a compound Henyey-Greenstein formula, Marcus (2007) also reviewed available information on backscattering and found from the data on seven comets that for phase angles from 0° to 30° the brightness decreases with increasing phase angle at an average rate of 0.031 ± 0.006 magnitude per degree. Since the phase angle at the end of the active phase of the megaburst was 16°.6, the slope fitted by Marcus provides for the comet's peak intrinsic magnitude a probable correction of -0.51 ± 0.10, so that $(H_0)_{peak}(corr) = -1.04 \pm 0.16$.

The phase could also affect the post-conjunction light curve of 17P/Holmes in the late 2008 and early 2009, as the phase angle reached a minimum of 2°.0 on 2009 January 27. This notion is supported by the fact that the comet was indeed fading very slowly, if at all, between October 2008 and early February 2009, as the phase angle decreased during this period of time by 12°, while the comet, more than 500 days after perihelion (Figure 1), continued to recede from the

sun. However, no measurable opposition effect is expected in this case, since the nucleus apparently contributed only a few percent to the comet's total light.

6. Modeling the Megaburst

The extreme steepness of brightness variations during the active phase of the megaburst and the lack of data in the early stage of the event limit one's options in modeling the temporal dust-injection profile. A technique of examination that has been applied and the results are presented in the following.

Except possibly in the earliest moments of the active phase, the expanding, sharply-bounded dust halo can safely be considered an optically thin medium (Sec. 8), so that its intrinsic brightness,

$$I_0(t) = 10^{-0.4H_0(t)}, \tag{1}$$

measures — for an assumed geometric albedo and phase effect (which is essentially constant during the very short active phase) — the total cross-sectional area of dust particles gradually accumulating in the expanding halo by a given time t, if the gas-coma contribution to the halo's visual brightness can be neglected. Via the dust-particle mass/size distribution function, the variations in $I_0(t)$ describe the rates at which the mass of the dust halo increased with time. If the mass-distribution law did not vary during the megaburst, then on the above assumptions the mass-injection rate, $d\mathcal{M}/dt$, should be proportional to the rate of intrinsic brightening,

$$\frac{d\mathcal{M}}{dt} = \frac{\mathcal{M}_0}{\Im_0}\frac{dI_0}{dt}, \tag{2}$$

where $\mathcal{M}_0 = 10^{14}$ g is the total mass of dust injected into the halo during the event (Table 3) and $\Im_0$ is the integrated intrinsic brightness of the halo at the time of termination of the active phase,

$$\Im_0 = \int_{t_{\rm beg}}^{t_{\rm end}} \frac{dI_0}{dt}\, dt. \tag{3}$$

In practice, $\Im_0$ is the peak intrinsic brightness, because the comet's quiescent intrinsic brightness at the onset of the megaburst was only 0.0003 percent of the peak brightness, and therefore negligible except close to the very onset of the megaburst. Because the values of both $\mathcal{M}_0$ and $\Im_0$ are known, temporal variations in the relative mass-injection rate of dust and in the relative rate of intrinsic brightening can be fitted by the same expression. I will refer to

$$\frac{d\tilde{I}_0(t)}{dt} = \frac{1}{\Im_0}\frac{dI_0(t)}{dt} = \frac{1}{\mathcal{M}_0}\frac{d\mathcal{M}(t)}{dt} \tag{4}$$

simply as a *relative dust injection rate* and to its integral $\tilde{I}_0(t)$ as a *relative integrated dust injection rate* at the given time.

Modeling of these variations is further streamlined by replacing time t with a dimensionless temporal quantity τ, defined by requiring that the onset and termination of the megaburst take place, respectively, at $\tau_{\rm beg} = 0$ and $\tau_{\rm end} = 1$, implying for a *normalized dust injection rate* $d\tilde{I}_0/d\tau$ the boundary conditions

$$\left[\frac{d\tilde{I}_0(\tau)}{d\tau}\right]_{\tau_{\rm beg}} = \left[\frac{d\tilde{I}_0(\tau)}{d\tau}\right]_{\tau_{\rm end}} = 0, \tag{5}$$

which, together with the general condition

$$\frac{d\tilde{I}_0(\tau)}{d\tau} > 0 \quad \text{for} \quad \tau_{\rm beg} < \tau < \tau_{\rm end}, \tag{6}$$

must be satisfied by any law that is to fit the activity profile of the megaburst. In this system of variables, time t is related to τ by

$$t = t_{\rm beg} + \tau\,(t_{\rm end} - t_{\rm beg}). \tag{7}$$

The task is to find a reasonably simple expression for $d\tilde{I}_0/d\tau$, such that the *normalized integrated dust-injection rate*,

$$\tilde{I}_0(\tau) = \int_0^{\tau} \frac{d\tilde{I}_0(\tau)}{d\tau}\, d\tau, \tag{8}$$

giving $\tilde{I}_0(\tau_{\rm end}) = \tilde{\Im}_0 = 1$, fits satisfactorily the observed variations in the intrinsic magnitude H_0, presented in Figure 2. The task includes an independent verification of the times of onset and termination of the active phase of the megaburst.

The simplest model is of course the case of a constant injection rate during the event,

$$\frac{d\tilde{I}_0(\tau)}{d\tau} = \mathcal{A}_0, \tag{9}$$

where $\mathcal{A}_0 = 1$ in order to satisfy the normalization conditions. The practical consequence of this model is an abrupt change in the injection rate at both the onset and termination points. Figure 2 provides no information on the nature of such a change at the onset ($\tau = 0$) but both Figure 2 and Figure 3 show that the transition to the plateau is fairly smooth. Thus, model (9) fails to provide a good approximation to the normalized injection-rate variations and a more complex law is needed.

Since a linear law,

$$\frac{d\tilde{I}_0(\tau)}{d\tau} = \mathcal{A}_0 + \mathcal{A}_1\tau, \tag{10}$$

does not satisfy simultaneously the boundary conditions (5) and the condition (6), one proceeds to the next possible approximation, a quadratic law,

$$\frac{d\tilde{I}_0(\tau)}{d\tau} = \mathcal{A}_0 + \mathcal{A}_1\tau + \mathcal{A}_2\tau^2. \tag{11}$$

The first boundary condition (5) requires that $\mathcal{A}_0 = 0$, with which the second condition is satisfied when $\mathcal{A}_1 = -\mathcal{A}_2 = \mathcal{A} > 0$, that is,

$$\frac{d\tilde{I}_0(\tau)}{d\tau} = \mathcal{A}\ \tau(1-\tau). \tag{12}$$

This law, used in my earlier investigation (Sekanina 2002) of the peculiar light curve of comet C/2002 O1 (Hönig), is symmetrical with respect to both ends of the event, with the peak occurring at $\tau_{\rm mid} = \frac{1}{2}$. The symmetry implies that $\tilde{I}_0(\tau_{\rm mid}) = \frac{1}{2}$ and that therefore $H_0(\tau_{\rm mid}) = (H_0)_{\rm peak} + 0.75 = +0.22$.[2] If the event lasted from 172.2 days to 174.4 days after perihelion (Table 3 or Paper 1), it is apparent from Figure 2 that $H_0(\tau_{\rm mid}) \simeq -0.2$ to -0.3 and that therefore the dust halo was then about 0.5 magnitude brighter. This discrepancy is diagnostic of an injection-rate curve that peaks in the first half of the active phase of the megaburst; an asymmetrical law thus needs to be introduced.

Heuristically, asymmetries can be incorporated into law (12) by introducing exponents $\mu > 0$ and $\nu > 0$ in one of two ways. The first option provides for the injection rate an expression

$$\frac{d\tilde{I}_0(\tau)}{d\tau} = \mathcal{A}\ \tau^{\mu}(1-\tau^{\nu}), \tag{13}$$

which is referred to as *Law I*, when μ and ν are not both unity. Integrating the injection rate from the onset of the megaburst to a point in the active phase described by τ, one obtains

$$\tilde{I}_0(\tau) = \tau^{1+\mu}\left[1 + \frac{1+\mu}{\nu}(1-\tau^{\nu})\right], \tag{14}$$

after setting from the normalizing condition

$$\mathcal{A} = \frac{(1+\mu)(1+\mu+\nu)}{\nu}. \tag{15}$$

The peak injection rate during the active phase,

$$\left(\frac{d\tilde{I}_0}{d\tau}\right)_{\rm peak} = \frac{(1+\mu)(1+\mu+\nu)}{\mu+\nu}\left(\frac{\mu}{\mu+\nu}\right)^{\mu/\nu}, \tag{16}$$

is reached at

$$\tau_{\rm peak} = \left(\frac{\mu}{\mu+\nu}\right)^{1/\nu}. \tag{17}$$

The constraint implied by the observations, $\tau_{\rm peak} < \frac{1}{2}$, requires that

$$\mu < \frac{\nu}{2^{\nu}-1}. \tag{18}$$

[2]The term (usually a subscript) *peak* is being employed in two meanings. From Sec. 3 on, it has been used in reference to the curve of intrinsic magnitude variations, with $(H_0)_{\rm peak}$ depicting the maximum brightness. From this section on, the term *peak* is also applied in reference to the curve of dust-injection rate in the active phase of the megaburst, with, *e.g.*, $(d\tilde{I}_0/d\tau)_{\rm peak}$ denoting the maximum normalized rate and $\tau_{\rm peak}$ its position within the event's boundaries. The author is content that the two usages of *peak* relate to quantities different enough to rule out a mixup.

For example, $\mu < 0.43$ when $\nu = 3$, $\mu < 1$ when $\nu = 1$, and $\mu < 1.21$ when $\nu = \frac{1}{2}$.

Comparison of a large set of models (14) with the observed light curve of the active phase of the megaburst in Figure 2 fails to yield a good match for any combination of μ and ν, thus prompting one to consider an alternative asymmetrical law.

An obvious way to proceed is to replace expression (13) for the injection rate with

$$\frac{d\tilde{I}_0(\tau)}{d\tau} = \mathcal{A}\,\tau^{\mu}(1-\tau)^{\nu}, \tag{19}$$

which is referred to as *Law II*, with the constraint as in (13). The integration now yields

$$\tilde{I}_0(\tau) = \frac{B_\tau(1+\mu, 1+\nu)}{B(1+\mu, 1+\nu)}, \tag{20}$$

where B_τ is the incomplete beta function to be calculated by numerical integration, while Euler's integral of the first kind, or the beta function, B, comes from the normalization,

$$\mathcal{A} = \frac{1}{B(1+\mu, 1+\nu)}, \tag{21}$$

and can be written in terms of the Γ function (Euler's integral of the second kind):

$$B(1+\mu, 1+\nu) = \frac{\Gamma(1+\mu)\;\Gamma(1+\nu)}{\Gamma(2+\mu+\nu)}. \tag{22}$$

To calculate the beta function, I use a polynomial approximation that matches the $\Gamma(x)$ function to better than 3×10^{-7} for any argument $0 < x \leq 1$. For arguments $x+n$, where n is a positive integer, $\Gamma(x+n)$ is given in terms of $\Gamma(x)$:

$$\Gamma(x+n) = \Gamma(x)\prod_{k=0}^{n-1}(x+k), \tag{23}$$

where Π is the product sign. Since negative values of μ and ν are irrelevant, so are arguments $x-n$. The peak injection rate

$$\left(\frac{d\tilde{I}_0}{d\tau}\right)_{\text{peak}} = \frac{\mu^{\mu}\nu^{\nu}}{(\mu+\nu)^{\mu+\nu}B(1+\mu, 1+\nu)} \tag{24}$$

is attained at

$$\tau_{\text{peak}} = \frac{\mu}{\mu+\nu}. \tag{25}$$

The constraint $\tau_{\text{peak}} < \frac{1}{2}$ is now equivalent to a simple condition $\mu < \nu$.

Experimentation with Law II models has shown that the observed integrated injection rate can be fitted, if the exponents μ and ν are allowed to greatly exceed unity. No least-squares solution has been attempted, but several models with different pairs of μ and ν have visually matched the observed intrinsic brightness variations during the active phase quite satisfactorily. One of the best fits, with $\mu = 8.0$ and $\nu = 11.5$, is exhibited in Figure 4, referring to the active phase that extends from 172.2 days to 174.4 days after perihelion. A more-detailed discussion of the effects of chosen parameters μ, ν, t_{beg}, and t_{end} on the H_0 curve is deferred to the end of this section, after I present the implications of the adopted fit for the variations in the dust-injection rate.

The most important physical information that can be derived from the fit in Figure 4 is a temporal profile of the mass-injection rate of dust during the active phase of the megaburst. Using (4), one can write

$$\frac{d\mathcal{M}(t)}{dt} = \mathcal{M}_0\,\frac{d\tilde{I}_0(\tau)}{d\tau}\,\frac{d\tau}{dt}. \tag{26}$$

Inserting for $d\tilde{I}_0(\tau)/d\tau$ from (19), (21), and (22), for τ and $d\tau/dt$ from (7), and rearranging the expression, one finds

$$\frac{d\mathcal{M}(t)}{dt} = \mathcal{M}_0\,\frac{(t-t_{\text{beg}})^{\mu}(t_{\text{end}}-t)^{\nu}}{(t_{\text{end}}-t_{\text{beg}})^{1+\mu+\nu}}\,\frac{\Gamma(2+\mu+\nu)}{\Gamma(1+\mu)\;\Gamma(1+\nu)}. \tag{27}$$

With $\mathcal{M}_0 = 10^{14}$ g, $t_{\text{beg}} = 172.2$ days, $t_{\text{end}} = 174.4$ days, and with exponents $\mu = 8.0$ and $\nu = 11.5$ of Law II, the mass injection rate of dust (in g/s) becomes

$$\frac{d\mathcal{M}(t)}{dt} = 2.22 \times 10^{8}\;(t-172.2)^{8}\;(174.4-t)^{11.5}, \tag{28}$$

where time t is again in days from perihelion. This model of dust-injection rate, plotted in Figure 5, predicts that the peak mass rate of 2.0×10^9 g/s, an extremely high value, occurred at $t_{peak} = 173.10$ days after perihelion, or on October 24.60 UT, by which time the megaburst was under observation for nearly 16 hours. The FWHM (full-width-at-half-maximum) of the injection-rate distribution curve is only 13.7 hours, from October 24.33 to 24.90 UT.

◇ ◇ ◇

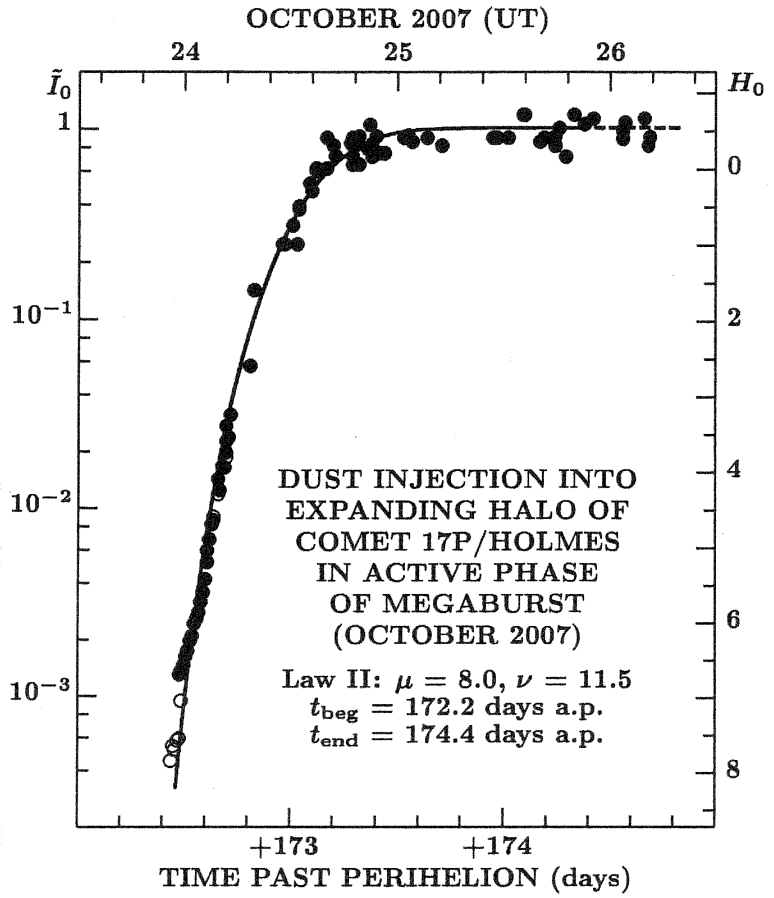

Figure 4. Curve of intrinsic brightness of comet 17P/Holmes during the active phase of the megaburst, rearranged as a plot of the normalized integrated dust injection rate $\tilde{I}_0$, defined by Eq. (8), against time from perihelion. The data points, which now also include several entries from Henriquez Santana's (2008) frames with a saturated image (shown as open circles), are fitted with one of the best Law II trial-and-error models found; a.p. = after perihelion.

◇ ◇ ◇

In terms of the peak injection rate of dust, the megaburst dwarfs comet 1P/Halley (even its 1836 explosion; cf. Paper 2) and competes favorably with the giant comet C/1995 O1 (Hale-Bopp), for which the peak dust-emission rate *at perihelion*, 0.91 AU from the sun, was found to be 4.6×10^8 g/s from mid-infrared measurements (Lisse *et al.* 1997) and 2×10^9 g/s from sub-millimeter measurements (Jewitt and Matthews 1999). And although, in the early stages of the megaburst, the injection rate is orders of magnitude lower than at the peak and increases very gradually in Figure 5, the model predicts that, at the time of first detection on October 23.945 UT (Henriquez Santana 2008), nearly 6 hours after the nominal onset, the mass rate was a respectable 6.4×10^6 g/s, and that the halo already contained nearly 2×10^{10} g of dust. Given the extremely feeble activity of comet 17P/Holmes in its quiescent phase, these numbers were more than sufficient to make the expanding halo detectable.

Finally, a few words about Law I vs. Law II and about the choice of the parameters μ, ν, t_{beg}, and t_{end}. All Law I models showed — for a wide range of (μ, ν) combinations and plausible values of t_{beg} and t_{end} — an unacceptably steep slope in the intrinsic magnitude near the end of the active phase relative to the slope in the first half of the event in Figure 4. Some Law II models with low values of μ and ν (generally near unity) could fit the late portion of the H_0 curve fairly well but failed completely for times prior to the peak in Figure 5, yielding slopes that were considerably less steep than indicated by the observations in Figure 4. Changing t_{beg} to an earlier time by more than 0.1 day caused most Law II models to run way above the data points. Those that did not could not fit the "knee" at the end of the steep slope. Choosing $t_{beg} = 172.3$ days after perihelion instead of 172.2 days resulted in models that visually fitted the data set nearly equally well, but increasing t_{beg} further caused the calculated curve to be too steep in the region of faint magnitudes. Thus, the onset time could actually be determined with greater accuracy than suggested by the mean error of ± 0.2 day from halo expansion. On the other hand, the quality of fit was much less sensitive to the time of termination of the active phase, t_{end}, whose determination from information on the post-megaburst plateau could not be improved.

◇ ◇ ◇

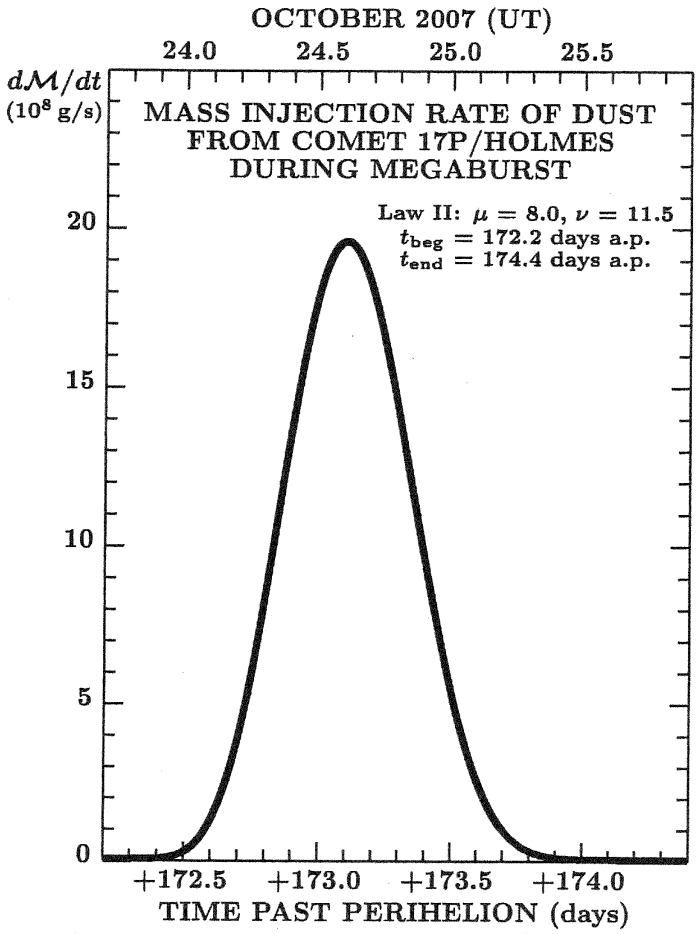

Figure 5. Variations in the dust injection rate from the nucleus of comet 17P/Holmes into the halo during the active phase of the megaburst. The injection curve is asymmetrical, reaching a peak at 0.41 the event's duration from the onset, at 173.10 days after perihelion, or on October 24.60 UT. The peak mass-injection rate of dust is equal to 2×10^9 g/s.

◇ ◇ ◇

7. Evidence for a Precursory Eruption

The curve of exceptionally rapid brightening during the active phase, whose fit in Figure 4 has been classified as quite satisfactory in Sec. 6, shows that the comet's intrinsic brightness on the faintest unsaturated images, with H_0 between 6.7 and 5.9, increases less steeply with time than on the subsequent images. The Law II fit in Figure 4 was chosen to smooth this potential discrepancy, which at first sight may appear to be almost within the errors of observation and therefore unimportant. By varying the parameters μ and ν, numerous models are found, each of which provides a virtually perfect fit to all data points brighter than $H_0 = 5.9$, in a period of time from about 172.6 days after perihelion (or October 24.1 UT) to the very end of the active phase, covering 82 percent of its span. However, once the fit to the steepest part of the observed H_0 curve is improved over the fit in Figure 4, the deviations of the magnitudes from the earliest observations (fainter than $H_0 \simeq 5.8$) become a little more apparent, such models running about 1 magnitude or more below the observations at 172.5 days after perihelion (October 24.0 UT). The predicted slope of a Law II curve is

$$\frac{dH_0(t)}{dt} = \frac{d}{dt}\left[-2.5 \log_{10} I_0(t)\right] = -\frac{2.5 \log_{10} e}{t_{\rm end} - t_{\rm beg}} \, \frac{1}{\tilde{I}_0(\tau)} \, \frac{d\tilde{I}_0(\tau)}{d\tau} = \text{const.} \, \frac{\tau^\mu (1-\tau)^\nu}{B_\tau(1+\mu, 1+\nu)}, \tag{29}$$

where the constant equals -0.02056 when the slope dH_0/dt is expressed in magnitudes per hour and the duration of the active phase is taken to be 2.2 days (Table 3). The limit for $t \to t_{\rm beg}$ is derived by applying L'Hôpital's rule,

$$\lim_{t \to t_{\rm beg}} \frac{dH_0(t)}{dt} \sim -\lim_{\tau \to 0+} \frac{\tau^\mu (1-\tau)^\nu}{B_\tau(1+\mu, 1+\nu)} \sim -\lim_{\tau \to 0+} \frac{1}{\tau} \cdot \left(\mu - \frac{\nu\tau}{1-\tau}\right) = -\infty. \tag{30}$$

Thus, the predicted slope at the event's onset is infinitely steep. In practice, because the comet's brightness at onset was not zero, the slope is finite, but the decreasing steepness of the H_0 curve with time that Law II models predict appears to be in conflict with the segment of the observed curve based on the earliest observations of the megaburst.

To investigate this contradiction more closely, I compare, in Table 4, the values for the slope dH_0/dt predicted by the nominal model from Figure 4 with the values derived from the photometric observations by Henriquez Santana (2008), by Trigo-Rodríguez *et al.* (2008), and by Hsieh *et al.* (2007). For the first four entries in Table 4, the observed slope is distinctly less steep, by a factor of 2 or more, than the slope predicted from the model in Figure 4. The times involved are 172.49 to 172.60 days after perihelion (October 23.99-24.10 UT). The last four entries show a better agreement between observation and model.

Table 4. Predicted and observed slopes of the curve of the intrinsic magnitude H_0 of comet 17P/Holmes early in the active phase of the megaburst.

Interval of time covered by data 2007 (UT)	Slope dH_0/dt (mag/hr)		Number of data used	Span of H_0 (mag)	Reference to observations
	predicted span	from data			
Oct. 23.99–24.10	−1.17 to −0.77	−0.42	2	6.7 to 5.6	Hsieh *et al.* (2007)
Oct. 24.00–24.02	−1.12 to −1.03	-0.50 ± 0.05	57	6.7 to 6.4	Henriquez Santana (2008)
Oct. 24.02–24.04	−1.03 to −0.96	-0.43 ± 0.06	48	6.5 to 6.2	Henriquez Santana (2008)
Oct. 24.04–24.08	−0.96 to −0.83	-0.36 ± 0.07	16	6.3 to 5.9	Henriquez Santana (2008)
Oct. 24.08–24.11	−0.83 to −0.74	-0.67 ± 0.07	13	5.9 to 5.4	Henriquez Santana (2008)
Oct. 24.11–24.14	−0.74 to −0.67	-0.79 ± 0.13	7	5.3 to 4.8	Henriquez Santana (2008)
Oct. 24.12–24.20	−0.72 to −0.56	-0.57 ± 0.01	4	5.0 to 3.9	Trigo-Rodríguez *et al.* (2008)
Oct. 24.18–24.23	−0.59 to −0.51	-0.82 ± 0.08	5	4.2 to 3.2	Trigo-Rodríguez *et al.* (2008)

Note. Usage of Henriquez Santana's (2008) data has been limited to frames with unsaturated images.

◇ ◇ ◇

This discrepancy may be used to argue that the heuristic Law II paradigm is inappropriate for fitting the variations in the integrated dust-injection rate during the megaburst. This is possible but unlikely, given that the nominal model applied in Figure 4 (and a number of similar models) provides an excellent fit to the observations over 82 percent of the event's active phase, while the disparity is seen over only 5 percent.

A better explanation is offered by proposing that the megaburst consisted of two components: a minor or moderate precursory eruption followed in rapid succession — and partially overlapped — by the powerful main event. Indeed, the flatter segment of the H_0 curve between October 23.99 and 24.10 UT in Figure 4 appears — in terms of the slope steepness — like a scaled-down portion of the same curve below the "knee", near 172.8 days after perihelion (October 24.3 UT) and H_0 = 2-3. This suggests that the paradigm from Sec. 6 should be expanded to include a model that describes the megaburst as a double-eruption event. The dust-injection rate is now to follow a compound law,

$$\frac{dI_0(t)}{dt} = \mathcal{Z}(t - t_{\rm beg})^{\mu}(t_{\rm end} - t)^{\nu} + \mathcal{Z}'(t - t'_{\rm beg})^{\mu'}(t'_{\rm end} - t)^{\nu'}, \tag{31}$$

where time t satisfies, as before, the condition $t_{\rm beg} \le t \le t_{\rm end}$ for the main eruption, with a new condition, $t'_{\rm beg} \le t \le t'_{\rm end}$, for the precursor whose eruption parameter $\mathcal{Z}'$ is much smaller than the main event's eruption parameter $\mathcal{Z}$. The parameters μ' and ν' are generally different from, respectively, μ and ν.

◇ ◇ ◇

Table 5. Parameters for the 2007 megaburst of comet 17P/Holmes modeled as a double-eruption event.[a]

Parameter	Precursory eruption	Main eruption
Time of onset (days after perihelion)	172.14	172.20
Date of onset (2007 UT)	October 23.64	October 23.70
Time of termination (days after perihelion)	172.74	174.40
Date of termination (2007 UT)	October 24.24	October 25.90
Duration (days)	0.6	2.2
Peak intrinsic magnitude (mag)	7.0	−0.53
Amplitude relative to quiescent phase (mag)	6.3	13.8
Mass of dust injected into the halo (g)	10^{11}	10^{14}
Time of peak dust-injection rate (days after perihelion)	172.38	173.07
Date of peak dust-injection rate (2007 UT)	October 23.88	October 24.57
Peak mass injection rate of dust (g/s)	8×10^6	2.2×10^9

[a] The values of the parameters μ' and ν' for the precursor and μ and ν for the main event have been searched on the assumption that their values are eruption independent; the best fit has been achieved when $\mu = \mu' = 9.4$ and $\nu = \nu' = 14.3$.

◇ ◇ ◇

A practical solution follows the approach described in Sec. 6 in that the two eruptions are treated separately until they have been normalized. Their contributions to the total mass of dust injected into the halo are determined by the respective peak intrinsic magnitudes, $(H'_0)_{\rm peak}$ for the precursor and, as before, $(H_0)_{\rm peak}$ for the main event. Once formulated, the problem can be solved by fitting the data by trial and error, just like in the nominal case (Figure 4).

Because insufficient information is available for 17P to determine a complete set of the precursor's parameters, reasonable assumptions must be introduced.

Improved fitting of the observations before October 24.1 UT by a double-eruption dust-injection model is illustrated by comparing Figure 4 with Figure 6. The parameters of the two eruptions are listed in Table 5. To make the solution tractable, I have assumed the same normalized profile of dust injection by requiring that $\mu' = \mu$ and $\nu' = \nu$ and searched for the best common values. An excellent match has been achieved by choosing μ and ν still greater than for the nominal model in Figure 4. The precursory event is found to have begun about $1\frac{1}{2}$ hours before the main eruption and to have ceased $\sim$ 13 hours after the latter's onset. Because this is only a model, it is academic to speculate about the fractions of the dust mass injected by each eruption during the period of overlap. The precursory eruption was apparently due to an early fragment, about 0.1 percent of the mass of the 10^{14} g that lifted from the nucleus' surface in its entirety — but not necessarily in one piece — a short time later. Indeed, for the physical scenario proposed in Paper 1 to work, precipitous fragmentation upon the liftoff was stated as a necessary condition, requiring that very large numbers of fragments like that causing the precursory event should have followed. However, as the comet was brightening dramatically, only the sum of these objects' contributions to the total injected mass — not the fleeting individual eruptions — is documented by the curve at $H_0 \lesssim 5.5$ in Figure 6.

◇ ◇ ◇

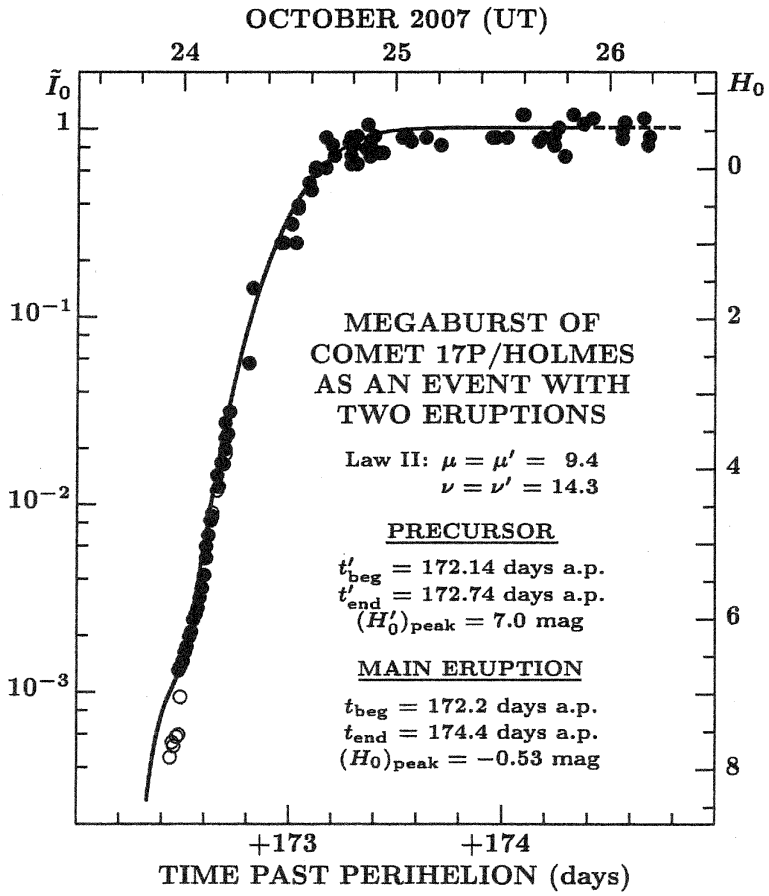

Figure 6. Curve of intrinsic brightness of comet 17P/Holmes during the megaburst, fitted as a double-eruption event. The precursor, a relatively minor outburst, is followed and overlapped by the main eruption. The precursor is responsible for a wiggle in the slope of the curve near the faintest magnitude data based mostly on Henriquez Santana's (2008) frames with unsaturated images. The primary parameters of the two eruptions are listed; for more information, see Table 5 and the caption to Figure 4.

◇ ◇ ◇

The curve of dust-injection rate offered by the double-eruption scenario is not displayed. The injection-rate variations for the main event closely follow the curve plotted in Figure 5, while those for the precursor would show up as a barely visible wiggle near the bottom left corner of the box in that figure. Both curves can be visualized from the eruption parameters in Table 5. I may add that the mass injection rate from the precursory eruption is predicted to have dominated until almost 172.42 days after perihelion (October 23.92 UT) and that the total mass of injected dust from the precursory eruption is found to have prevailed until almost 172.53 days after perihelion (October 24.03 UT), when it was overtaken by the integrated contribution from the main event. At the latter time, the comet was under observation by Henriquez Santana (2008) and by Hsieh *et al.* (2007).

I conclude that the precursory eruption provides compelling evidence for the existence of an early disintegrating fragment — and, by extension, for an impending large number of similar objects whose liftoff and continuing crumbling were the source of the main event, thereby strongly supporting the physical scenario proposed in Paper 1. Comparison of Figures 4 and 6 shows that introducing the precursor improved noticeably the fit to the observations in the span of faint intrinsic magnitudes. An additional piece of supporting evidence is provided by Henriquez Santana's (2008) saturated

images taken between October 23.945 and 23.999 UT, at times before his first frames with unsaturated images were obtained and mostly before Hsieh *et al.*'s (2007) imaging commenced. The only value of saturated images is in that they offer a lower limit to the comet's brightness. It is significant that this expectation is satisfied by the double-eruption model from Figure 6 but not by the nominal model from Figure 4.

8. Optical Depth

Because of the enormous amounts of dust injected into the halo during the active phase of the megaburst in general and a significant contribution from microscopic particles in particular, the optical depth of the dust cloud should at least crudely be examined. Since the expanding halo was getting ever thinner once the active phase terminated, it suffices to investigate only the time while the megaburst lasted. With the temporal profile of the dust-injection rate established, I am in a position to address two issues: a *mean* optical depth of the halo and an extent of its optically thick central region.

Let J_0 be a flux impinging on the sharply-bounded halo, whose dimensions and cross-sectional area, $X_{\rm halo}$, are determined by the rate of expansion. After passing through the cloud of dust that makes up the halo, this flux is attenuated to $J < J_0$. The degree of attenuation varies as the total area obscured by dust particles in the cloud. In the absence of moderate-to-high opacity,[3] this area is approximately equal to the sum $X_{\rm dust}$ of cross-sectional areas of all dust particles present in the halo. From its definition, the mean optical depth χ of the halo is

$$\frac{J}{J_0} = \exp(-\chi), \tag{32}$$

where

$$\begin{aligned} J_0 &= \zeta\ X_{\rm halo}, \\ J &= \zeta\ X_{\rm halo} - \zeta\kappa\ X_{\rm dust}, \end{aligned} \tag{33}$$

ζ is a constant of proportionality, and $\kappa \leq 1$ is a coefficient introduced here in order that a dust cloud of high opacity conforms to the same formalism. The mean optical depth at time t is from Eqs. (32) and (33)

$$\chi(t) = -\ln\left[1 - \kappa\ \frac{X_{\rm dust}(t)}{X_{\rm halo}(t)}\right], \tag{34}$$

where I take $\kappa = 1$ when $X_{\rm dust} \leq X_{\rm halo}$, but $\kappa = X_{\rm halo}/X_{\rm dust} < 1$ when $X_{\rm dust} > X_{\rm halo}$ (a case of extremely high opacity). This warrants that the expression in the brackets is always positive or zero; when it is zero, $\chi \rightarrow \infty$. When $X_{\rm dust} \ll X_{\rm halo}$, $\chi \doteq X_{\rm dust}/X_{\rm halo}$. Equation (34) could be refined by replacing the geometric cross-sectional areas of dust grains with their absorption and scattering cross-sectional areas, accounting for multiple scattering, etc., but this is unnecessary given that other approximations (e.g., a temporally invariable particle-size distribution) allow one to get only an order-of-magnitude estimate for the optical depth.

The cross-sectional area of a uniformly expanding halo at time t is

$$X_{\rm halo}(t) = \pi v_{\rm exp}^2 (t - t_{\rm beg})^2, \tag{35}$$

where $v_{\rm exp}$ is its expansion velocity and $t_{\rm beg}$ is again the onset time of the active phase (Table 3). The total cross-sectional area X_0 of all dust particles injected into the halo by the end of the active phase, $t_{\rm end}$, is determined by Eq. (2) of Paper 1 as a function of a dimensionless variable $\Phi(\alpha)$, which depends on the phase angle α and is normalized to $\Phi(0°) = 1$. In Sec. 5 I noted that a likely phase correction at the end of the active phase was -0.51 mag, so that $\Phi = 10^{-0.51\times0.4} = 0.625$ and the total area of dust, in km^2, is

$$X_0 \equiv X_{\rm dust}(t_{\rm end}) = \frac{5.7 \times 10^7}{\Phi} = 9.1 \times 10^7. \tag{36}$$

Accordingly, the total cross-sectional area of dust particles injected into the halo by time t, where $t_{\rm beg} < t < t_{\rm end}$, is (from Sec. 6)

$$X_{\rm dust}(t) = X_0\ \tilde{I}_0(\tau), \tag{37}$$

where $\tau = (t - t_{\rm beg})/(t_{\rm end} - t_{\rm beg})$ from Eq. (7) and $\tilde{I}_0(\tau)$ from Law II is described by Eqs. (20) and (22).

---

[3] Opacity is an optical quantity that links a mean free path of light passing through a medium (in this case the halo) to the spatial density of the material (here the cloud of dust particulates). Passing light can get absorbed or scattered. If the mean free path is much greater than the dimensions of the medium, the optical depth is much lower than unity and the medium is optically thin. As the spatial density of the material increases, the optical depth increases and the medium may eventually become optically thick. The absorption and scattering cross-sectional areas of a microscopic dust particle depend on the optical properties of the material it is made of and they generally differ in a complex way from the particle's geometric cross-sectional area; for spherical particles the involved extinction coefficients are determined by the Mie solution to Maxwell's equations for scattering of electromagnetic radiation (usually referred to as the Mie theory).

Using t_{beg} and t_{end} from Table 3 and the nominal model's parameters $\mu = 8.0$ and $\nu = 11.5$ from Figure 4, and inserting from Eqs. (35), (36), and (37) into (34), one gets for the halo's mean optical depth the values listed in Table 6. It is seen that $\chi(t)$ does not exceed 0.01 for any t between t_{beg} and t_{end}, so that the halo as a whole is optically thin at all times.

◇ ◇ ◇

Table 6. Mean optical depth in the dust halo of comet 17P/Holmes during the 2007 megaburst.

Time from onset of event (days)	Time t from perihelion (days)	Mass injection rate of dust at time t (g/s)	Total mass of dust injected into halo by time t (g)	Cross-sectional area (10^6 km^2)		Mean optical depth, $\chi(t)$
				cloud of dust, $X_{dust}(t)$	expanding halo, $X_{halo}(t)$	
0.01	172.21	1.83×10^{-4}	1.77×10^{-2}	$\ll$0.0000001	0.586	$\ll$0.00000001
0.1	172.3	1.11×10^{4}	1.14×10^{9}	0.0000104	58.6	0.00000018
0.2	172.4	1.64×10^{6}	3.56×10^{9}	0.00324	235	0.000014
0.4	172.6	1.25×10^{8}	6.37×10^{11}	0.579	938	0.00062
0.7	172.9	1.35×10^{9}	1.73×10^{13}	15.8	2870	0.0055
1.0	173.2	1.80×10^{9}	6.39×10^{13}	58.1	5860	0.010
1.4	173.6	2.51×10^{8}	9.80×10^{13}	89.1	11500	0.0078
1.8	174.0	6.48×10^{5}	1.00×10^{14}	91.0	19000	0.0048
2.2	174.4	.....	1.00×10^{14}	91.0	28400	0.0032

◇ ◇ ◇

I now examine the conditions under which a central region of the halo becomes optically thick. I consider dust injections during a limited period of time, $t_{pre} \le t \le t_{now}$. The cross-sectional area of a corresponding region of the halo at time t_{now} is

$$\Delta X_{halo}(t_{pre}, t_{now}) = \frac{\pi}{4} D^2(t_{pre}, t_{now}), \tag{38}$$

where $D(t_{pre}, t_{now})$ is the diameter of this region at time t_{now}

$$D(t_{pre}, t_{now}) = 2\, v_{exp}(t_{now} - t_{pre}). \tag{39}$$

The total cross-sectional area of dust particles injected into the halo during the time period from t_{pre} to t_{now} is

$$\Delta X_{dust}(t_{pre}, t_{now}) = \frac{X_0}{\mathcal{M}_0} \left\langle \frac{d\mathcal{M}}{dt} \right\rangle \frac{D(t_{pre}, t_{now})}{2v_{exp}}, \tag{40}$$

where X_0 and $\mathcal{M}_0$ are given, respectively, by Eq. (36) and in Table 3, and $\langle d\mathcal{M}/dt \rangle$ is an average mass rate of dust injected into the halo between t_{pre} and t_{now}. From Eq. (34), an optical depth $\chi > 1$ is reached in this region at time t_{now} when

$$1 - \kappa \frac{\Delta X_{dust}(t_{pre}, t_{now})}{\Delta X_{halo}(t_{pre}, t_{now})} < \frac{1}{e}. \tag{41}$$

Rearranging (41), inserting from Eqs. (38) and (40), taking $\kappa \simeq 1$, and equating $D(t_{pre}, t_{now})$ with the diameter D_{thick} of an optically thick region around the nucleus, one gets for the latter a condition:

$$D_{thick} < 1.8 \times 10^{-6} \left\langle \frac{d\mathcal{M}}{dt} \right\rangle, \tag{42}$$

where D_{thick} is in km and $\langle d\mathcal{M}/dt \rangle$ in g/s. Using the peak mass-injection rate of dust, 2×10^9 g/s (Table 3), as an upper limit on $\langle d\mathcal{M}/dt \rangle$, one obtains a robust constraint on the diameter of the optically thick region:

$$D_{thick} < 3600 \text{ km}. \tag{43}$$

At the comet's geocentric distance of 1.64 AU, the optically thick region of the halo was less than 3″ in diameter in projection onto the plane of the sky, which is comparable to the seeing disk. Since the peak injection rate was reached on October 24.6 UT, or 0.9 day after the onset of the megaburst, the halo was at this time already 78,000 km in diameter and the optically thick region was less than 5 percent of the whole halo extent. This result suggests that between October 23.99 and 24.10 UT, or 0.29 to 0.40 day after the onset of the megaburst, when the SuperWASP-N facility observations were made, the diameter of the halo's optically thick central part was negligibly small, completely immersed in the seeing

disk. The rest of the halo, calculated to be 21″ to 29″ in diameter during this period of time, was optically thin, contrary to Hsieh *et al.*'s (2007) assumption used in their derivation of the onset time of the megaburst (Sec. 4).

It should be mentioned that the presented model for optical depth greatly simplifies the situation in the sense that the expansion velocity $v_{exp} = 0.50$ km/s is an upper limit on radial velocities of individual dust particles in the halo. Grains larger than a few microns in diameter move with lower velocities and therefore stay in the central region longer, thus increasing its optical depth. However, it is known that the optically-most-important dust consists of micron- and submicron-sized particles, which are responsible for the halo's observed expansion velocity. A preponderance of dust particles smaller than 0.6 μm in size has been proposed for the megaburst by Kiselev *et al.* (2008) as a likely explanation for an unusually low degree of negative polarization observed by them in the dust halo of comet 17/Holmes in late October and early November 2007. No major optical-depth effect is therefore expected from larger dust.

9. Conclusions

Examination of the 2007 post-perihelion light curve of comet 17P/Holmes, covering — with a conjunction gap — nearly two years at the time of this writing, demonstrates that, following the unprecedented explosion, the comet remained intrinsically very bright. A post-megaburst plateau, lasting for a period of at least six months, shows that the comet's light curve began very gradually, yet progressively, deviating from the light curve of a loss-free halo, representing a hypothetical case of no escaping dust. After conjunction with the sun, from the late 2008 on, the comet continued to be brighter by about 4 magnitudes, or a factor of 40, compared with a mean light curve from the 1986-2000 apparitions. In fact, some 600 days after the 2007 perihelion, the comet was intrinsically brighter than it had been 300 days after the 1993 perihelion.

After two major explosions in 1892-1893, the comet returned to the sun brighter in 1899 than in 1986-2000 and it underwent another outburst, with an amplitude of at least $3\frac{1}{2}$ magnitudes, in early July 1899, some 67 days after perihelion. Noticed here for the first time, that event was accompanied by no bright, expanding dust halo. When the outburst subsided, the comet remained — some 150-300 days after perihelion — at least 1.7 magnitudes, and possibly more than 2 magnitudes, brighter than in 1986-2000. Long after perihelion, the comet was about as bright at the poorly observed apparition of 1906 as in late 1899, suggesting that elevated activity lingered over at least two revolutions about the sun following the 1892-1893 events.

Based on its behavior at the 1892-1906 apparitions, comet 17P/Holmes is expected to show elevated activity at the forthcoming returns to the sun. It is estimated that the comet will reach apparent magnitude ~20 during its March 2011 near-aphelic opposition and it may acquire — at least for a few revolutions about the sun — the status of an "annual" comet, observable all around the orbit.

A phase correction, usually ignored in studies of cometary light curves, is given limited attention in this paper. Because of its large perihelion distance, comet 17P/Holmes can never be observed from the earth at phase angles greater than 28°. Effects of smaller phase angles, while not negligible, do not change our overall understanding of the comet's basic physical properties and evolution.

The early detection of the 2007 megaburst of comet 17P/Holmes has allowed one not only to determine the peak intrinsic magnitude, the amplitude, and the duration of this event — the results being very close to the preliminary values in Paper 1 — but also to model its evolution and temporal dust-emission variations during the active phase. The rate at which dust was injected into the expanding halo shows a sharp peak about 0.9 day after the onset of the megaburst, or on October 24.6 UT, when the mass-injection rate reached briefly 2×10^9 g/s, with a FWHM of less than 14 hours. This is comparable to the dust-production rate of the giant comet C/1995 O1 (Hale-Bopp) at perihelion, less than 1 AU from the sun! An average injection rate of dust during the megaburst comes out to be about 5×10^8 g/s, which compares with a peak total outgassing rate of 2×10^8 g/s, estimated for 17P/Holmes by Biver *et al.* (2008) from their radio observations on 2007 October 25.9 UT.

Large numbers of photometric observations that depict in detail the comet's dramatic brightening during the active phase of the megaburst have made it possible to improve the nominal, single-eruption model by investigating, for the first time, the possibility that the megaburst consisted of more than one eruption. Slight systematic differences between the observations and the nominal model at the lower end of the H_0 curve in Figure 4 can be removed if the main eruption followed a minor, precursory event. A compound law, introduced in Sec. 7, incorporates the precursor into this proposed scenario and improves the fit to the observations for the times before 2007 October 24.1 UT, as shown in Figure 6. The precursor is found to have begun about $1\frac{1}{2}$ hours before the main eruption, its contribution to the total mass of dust injected into the halo is estimated at 0.1 percent, and its peak mass-injection rate is calculated to have amounted to about 8×10^6 g/s. The double-eruption model is also consistent with the constraints provided by Henriquez Santana's (2008) saturated images obtained between October 23.945 and 23.999 UT.

The precursory eruption is interpreted as a stamp of an early disintegating fragment's emanation from the nucleus of 17P/Holmes that signaled the imminent liftoff of 10^{14} grams of particulate material. It appears that, by extension, this main event may have consisted of a rapid sequence of a very large number of similar, almost simultaneous eruptions, which could not be temporally resolved and which imply an equally large number of fragments as their source. This scenario strongly supports the physical theory for the megaburst in Paper 1, which required precipitous crumbling of the mass of 10^{14} grams upon the liftoff.

Because of the large amounts of dust injected into the halo in the course of the megaburst, an optical depth in the halo has been calculated. The mean optical depth is found not to exceed 0.01 at any time and an optically thick central region is restricted to a diameter of a few arcseconds or less, comparable at most to the dimensions of a seeing disk. It is concluded that the dust halo essentially behaved as an optically thin medium.

The megaburst of 17P/Holmes has offered the first opportunity to study the morphology of a short-lived explosive event experienced by a comet and to distinguish among different models to describe it. Hopefully, it will be possible, thanks in part to an increasing number of robotic imaging facilities being currently set up into operation worldwide, to test such activity from other comets in the near future.

Acknowledgements

I am grateful to J. A. Henriquez Santana for providing me with an extensive account of his observations of 17P/Holmes from the night of 2007 October 23/24. I thank D. W. E. Green for reading the manuscript of this paper and for his remarks and editorial work. I also thank B. G. Marsden for his comments and information. This research was carried out at the Jet Propulsion Laboratory, California Institute of Technology, under a contract with the National Aeronautics and Space Administration.

REFERENCES

Aitken, R. G. (1900). "Observations of Holmes's Comet 1899 II", *Astron. Nachr.* **151**, 29-30.

Backhouse, T. W. (1902). "Comets", *Publ. West Hendon House Obs.* No. 2, pp. 47-97.

Balam, D. D.; and J. B. Tatum (1993). "Observations of Comets: Periodic Comet Holmes", *Minor Planet Circ.* 22717.

Barnard, E. E. (1896). "Photographic and Visual Observations of Holmes' Comet", *Astrophys. J.* **3**, 41-46.

Barnard, E. E. (1913). "Comet III 1892 (Holmes)", *Publ. Lick Obs.* **11**, 26-31.

Barnard, E. E. (1932). "Observations of Comets (I)", *Astron. J.* **41**, 145-167.

Biver, N.; D. Bockelée-Morvan; H. Wiesemeyer; J. Crovisier; R. Peng; D. Lis; T. Phillips; J. Boissier; P. Colom; E. Lellouch; and R. Moreno (2008). "Composition and Outburst Follow-Up Observations of Comet 17P/Holmes at the Nançay, IRAM, and CSO Radio Observatories", in *Asteroids, Comets, Meteors 2008*, LPI Contr. No. 1405, Paper 8146.

Bobrovnikoff, N. T. (1943). "The Periodic Comet Holmes (1892 III)", *Pop. Astron.* **51**, 542-551.

Copeland, R. (1893). "Weitere Mitteilungen über den Cometen 1892 . . . (Holmes Nov. 6). Auszug aus Edinburgh Circular Nr. 32", *Astron. Nachr.* **131**, 133-134.

Divine, N.; H. Fechtig; T. I. Gombosi; M. S. Hanner; H. U. Keller; S. M. Larson; D. A. Mendis; R. L. Newburn; R. Reinhard; Z. Sekanina; and D. K. Yeomans (1986). "The Comet Halley Dust and Gas Environment", *Space Sci. Rev.* **43**, 1-104.

Gibson, J. (1986). "Periodic Comet Holmes (1986f)", *IAU Circ.* 4225.

Guido, E.; G. Sostero; and M. Suzuki (2007). "Observations of Comets", *Minor Planet Electr. Circ.* 2007-K18.

Hasubick, W. (2009). "Observations of Comets", *Minor Planet Electr. Circ.* 2009-E06.

Henriquez Santana, J. A. (2007). "Comet 17P/Holmes", *IAU Circ.* 8886.

Henriquez Santana, J. A. (2008). Personal communication.

Holmes, E. (1892). "Discovery of a New Comet in Andromeda", *Observatory* **15**, 441-443.

Hsieh, H. H.; A. Fitzsimmons; and D. L. Pollacco (2007). "Comet 17P/Holmes", *IAU Circ.* 8897.

Jäger, M. (2000). "Die fotografische Kometenbeobachtungen: Komet 17P/Holmes", *Schweifstern* **16**, No. 88, p. 20.

Jewitt, D.; and H. Matthews (1999). "Particulate Mass Loss from Comet Hale-Bopp", *Astron. J.* **117**, 1056-1062.

Kiselev, N.; V. Rosenbush; S. Velichko; F. Velichko; L. Kolokolova; and K. Antoniuk (2008). "Unusual Polarization During Outburst of Comet 17P/Holmes", in *Asteroids, Comets, Meteors 2008*, LPI Contr. No. 1405, Paper 8124.

Kobold, H. (1893). "Beobachtungen des Cometen 1892 III (Holmes)", *Astron. Nachr.* **132**, 303-304.

Leisy, P. (1999). "Observations of Comets: 17P/Holmes", *Minor Planet Circ.* 34696.

Lisse, C. M.; Y. R. Fernández; M. F. A'Hearn; T. Kostiuk; T. A. Livengood; H. U. Käufl; W. F. Hoffmann; A. Dayal; M. E. Ressler; M. S. Hanner; G. G. Fazio; J. L. Hora; S. B. Peschke; E. Grün; and L. K. Deutsch (1997). "Infrared Observations of Dust Emission from Comet Hale-Bopp", *Earth Moon Plan.* **78**, 251-257.

Marcus, J. N. (2007). "Forward-Scattering Enhancement of Comet Brightness. I. Background and Model", *Int. Comet Quart.* **29**, 39-66.

Marsden, B. G. (1973). "Comets in 1972", *Quart. J. Roy. Astron. Soc.* **14**, 389-406.

Marsden, B. G. (1985). "Comets in 1978", *Quart. J. Roy. Astron. Soc.* **26**, 92-105.

McCrosky, R. E.; C.-Y. Shao; G. Schwartz; J. Bulger; and E. Fogelin (1980). "Observations Made at the Harvard College Observatory Agassiz Station", *Minor Planet Circ.* 5298.

Nakamura, A. (1993). "Observations of Comets: Periodic Comet Holmes", *Minor Planet Circ.* 22717.

Nakamura, A. (1994). "Tabulation of Comet Observations: Periodic Comet Holmes (1993i)", *Int. Comet Quart.* **16**, 20.

Oribe, T. (2001). "Observations of Comets: 17P/Holmes", *Minor Planet Circ.* 42661.

Perrine, C. D. (1899). "Rediscovery and Observation of Holmes's Comet d 1899 = 1892 III", *Astron. J.* **20**, 72.

Perrine, C. D. (1900). "Observations of Holmes's Periodic Comet 1899 II", *Astron. J.* **20**, 187-188.

Roemer, E. (1971). "Periodic Comet Holmes (1971b)", *IAU Circ.* 2338.

Roemer, E. (1973). "Comet Notes", *Mercury* **2**, No. 3, pp. 17-19.

Roemer, E. (1981). "Observations of Comets: Periodic Comet Holmes", *Minor Planet Circ.* 5864.

Roemer, E.; and R. E. Lloyd (1966). "Observations of Comets, Minor Planets, and Satellites", *Astron. J.* **71**, 443-457.

Scotti, J. V. (1987). "Tabulation of Comet Observations: Periodic Comet Holmes (1986f)", *Int. Comet Quart.* **9**, 120.

Sekanina, Z. (2002). "What Happened to Comet 2002 O4 (Hönig)?", *Int. Comet Quart.* **24**, 223-236.

Sekanina, Z. (2008a). "Exploding Comet 17P/Holmes", *Int. Comet Quart.* **30**, 3-28. (Paper 1.)

Sekanina, Z. (2008b). "On a Forgotten 1836 Explosion from Halley's Comet, Reminiscent of 17P/Holmes' Outbursts", *Int. Comet Quart.* **30**, 63-74. (Paper 2.)
Seki, T. (1993). "Periodic Comet Holmes (1993i)", *IAU Circ.* 5804.
Shao, C.-Y.; and G. Schwartz (1979). "Periodic Comet Holmes (1979f)", *IAU Circ.* 3384.
Trigo-Rodríguez, J. M.; B. Davidsson; P. Montañés-Rodríguez; A. Sánchez; and B. Troughton (2008). "All-Sky Cameras Detection and Telescope Follow-Up of the 17P/Holmes Outburst", in *Lunar and Planetary Science Conference XXXIX*, LPI Contr. No. 1391, p. 1627.
Wolf, M. (1892). "Die Anzahl der Sterne auf einigen photographischen Aufnahmen", *Astron. Nachr.* **129**, 321-324.
Wolf, M. (1906a). "Auffindung des Holmesschen Kometen 1906f", *Astron. Nachr.* **172**, 223-224.
Wolf, M. (1906b). "Photographische Aufnahmen von kleinen Planeten und Kometen", *Astron. Nachr.* **172**, 255-256.
Wolf, M. (1906c). "Photographische Aufnahmen des Holmesschen Kometen und kleiner Planeten", *Astron. Nachr.* **172**, 301-302.
Wolf, M. (1906d). "Photographische Beobachtungen des Holmesschen Kometen", *Astron. Nachr.* **172**, 357-358.
Wolf, M. (1906e). "Photographische Aufnahmen des Holmesschen Kometen und kleiner Planeten", *Astron. Nachr.* **172**, 359-360.
Wolf, M. (1907). "Photographische Beobachtungen von Kometen", *Astron. Nachr.* **173**, 303-304.

Φ Φ Φ

Fourth and Fifth Workshops On Cometary Astronomy

Further to the preliminary announcement in the April 2008 issue of the *ICQ* (p. 63), we are now planning to hold the fourth IWCA at the Science and Technology Museum in Shanghai, China, on 2009 July 23 (Thursday) – one day after the long total solar eclipse of 2009 July 22 (totality will be visible in Shangai, weather permitting). As of late March 2009, cometary enthsiasts from at least eight countries outside of Asia have indicated their attention to attend this meeting. Additional details will appear at the *ICQ* website (where a webpage devoted to the IWCA IV exists) as soon as they become available. Please contact the *ICQ* Editor if you would like to attend and/or give a talk.

Also, the IWCA V will occur only two weeks later, in Rio de Janeiro, Brazil, on 2009 August 8 (Saturday), at the time of the International Astronomical Union's triennial General Assembly there. The fifth IWCA is being organized jointly by the Ibero American Astronomy League (Liga Ibero Americana de Astronomia = LIADA) and the *ICQ* and — as is the purpose of the IWCA series — will include the participation of both professional and amateur astronomers. LIADA's Comets Section will also call this the Third Ibero American Symposium on Comets of LIADA. The meeting will be held at the Planetarium of Rio de Janeiro. On Aug. 7, the meeting of the Comets Section of the LIADA will be held at the same location and conducted in both Portuguese and Spanish languages. On Aug. 8, IWCA V will be conducted entirely in English. Again, a special webpage has been established for IWCA V at the *ICQ* website, with links to local websites in Brazil. Also, interested individuals may contact the Comets Section of LIADA by e-mail for additional information (`cometas@astronomiaonline.com`).

Φ Φ Φ

Photometry of Deep-Sky Objects

For explanation of the tabulated data below, see the explanation in the tabulated data on comets in the section following this section. The previous batch of photometry of *ICQ*-recommended deep-sky objects appeared in the Jan. 2008 issue, pp. 29-30. We encourage *all* regular *ICQ* contributors to contribute to this project; see the *ICQ* list of recommended deep-sky objects (*ICQ* **20**, 98; **16**, 129; and **26**, 3; also listed at the *ICQ* website).

◇ ◇ ◇

Visual Data

NGC 221

DATE (UT)	N	MM	MAG.	RF	AP.	T	F/	PWR	COMA	DC	TAIL	PA	OBS.
2008 08 09.00		M	9.1	TI	10.5	M	14	37	2.5	7			MARO2
2008 08 23.92		M	8.9	TI	10.5	M	14	37	3	6			MARO2
2008 08 30.92		M	7.7	TI	10.5	M	14	37	4	6			MARO2

NGC 6356

DATE (UT)	N	MM	MAG.	RF	AP.	T	F/	PWR	COMA	DC	TAIL	PA	OBS.
2008 08 23.88		S	8.8	TI	10.5	M	14	37	2	4			MARO2
2008 08 30.89		S	8.6	TI	10.5	M	14	37	3	2/			MARO2